ICAS PAPER NO. 72 – 26

CANADIAN SONIC BOOM SIMULATION FACILITIES

by
I. I. Glass, H. S. Ribner, and J. J. Gottlieb
University of Toronto, Canada

The Eighth Congress of the International Council of the Aeronautical Sciences

INTERNATIONAAL CONGRESCENTRUM RAI-AMSTERDAM, THE NETHERLANDS
AUGUST 28 TO SEPTEMBER 2, 1972

Price: 3. Dfl.

CANADIAN SONIC-BOOM SIMULATION FACILITIES

I.I. Glass*, H.S. Ribner* and J.J. Gottlieb†
Institute for Aerospace Studies
University of Toronto
Toronto, Canada

Abstract

In order to obtain Canadian-based data on psychoacoustic, physiological, and structural response to sonic boom, two major facilities were constructed at the Institute for Aerospace Studies. One is a loudspeaker-driven simulator which is able to mimic arbitrarily distorted sonic booms within a small booth; the other is a large horn-type simulator with a capability for generating powerful travelling-wave sonic booms of substantial spatial extent or duration. The horn and booth-type simulation facilities complement each other for the study of human, animal, and structural response to the sonic boom.

The loudspeaker-driven simulator is in the form of a solidly built booth about 2 cubic meters in volume (70 cubic feet), which can house a single seated subject. Owing to the flexibility of the electronic circuitry, features of the sonic-boom pressure signature therein can be adjusted at will. Thus, response to the variation of such characteristics as N-wave overpressure, rise time, and duration can be evaluated. Additionally, a variety of psychoacoustic studies can be performed with either transient or steady sounds. As a new feature, the signal can be predistorted by means of a special function generator to help cancel the loudspeaker distortion. The initial performance of the facility is reported.

The travelling-wave simulator horn is in the form of a concrete horizontal pyramid 24.4 meters in length (80 feet) with a 3.0 by 3.0 meter open base (10 by 10 feet). At the apex a specially-designed mass flow valve is used to generate sonic boom N-waves of suitable amplitude and duration, and acceptably-short rise times; alternatively, shock-tube drivers are used for generating short-duration sonic booms. The interior of the horn contains a high-frequency sound absorber to reduce undesirable jet noise, and the open end has a specially-designed reflection eliminator in the form of a recoiling porous piston. The initial performance is reported, together with advances in the gasdynamic analysis of such devices. In addition, some initial physiological test results are presented.

I. Introduction

The supersonic transport (SST) will probably be in service during the next ten years with prime operation over the North Atlantic and the possibility of flights over Northern Canada. Even though the latter is sparsely populated, it is far from being an empty land with its abundant wildlife. All forms of life within the sonic-boom corridors will be subjected to the boom. For this reason, independent and open data unique to the Canadian scene must be obtained before SST's are operational there. Such information is needed to help prepare accurate guidelines for new legislation that will govern flight paths as affected by Canadian weather, terrain, wildlife, and population distribution. Guidelines developed for other countries are helpful but of uncertain applicability. In order to gather domestic sonic-boom data, simulation facilities provide the most inexpensive method.

The initial sonic-boom program at UTIAS was started in 1969 utilizing the hypervelocity launcher laboratory for a preliminary investigation of the diffraction of a bow shock wave over a model of the new Toronto City Hall[1]. It was soon realized that if significant data were to be obtained on human, animal, and structural response, then more meaningful simulation facilities would have to be constructed for this specific purpose. Under the direction of Dr. I.I. Glass and Dr. H.S. Ribner, two sonic-boom simulation facilities were developed: a travelling-wave simulator based on the previous work done at the General Applied Science Laboratories (GASL)[2], and a loudspeaker-driven booth based on the initial work done at the Lockheed-California Company[3] and the University of Southampton[4]. Construction of the two facilities started in 1970, and relevant calibration and performance data were obtained in 1971.

The primary function of the small volume (2 m^3) loudspeaker-driven booth will be to study human response to transient signals such as the sonic boom, other impulsive sounds, industrial or transportation noise, or alternatively, steady signals. In addition, theoretical concepts concerning the loudness of the sonic boom or other transient sounds as a function of their frequency content can be explored by listening tests. These studies are just commencing. The present paper gives a description of the facility, its mode of operation, and presents preliminary examples of sonic-boom simulation.

The travelling-wave horn-type simulator can be used for human, animal, and structural response or damage studies. However, since the facility has the capability of generating powerful sonic booms it is particularly well-suited for structural studies (wall panels, windows, room resonance). Due to the travelling-wave nature of the simulated boom, studies can be made of wave diffraction over model buildings or wave propagation over different reduced-scale land topologies. The simulated sonic booms can be generated either by means of a shock-tube driver for short-duration waves, or by a gas reservoir and mass flow valve for long-duration waves. The travelling-wave simulator and its method of operation using the two different generators are described, and the relevant theory is developed.

II. The Loudspeaker-Driven Booth

Description

For psychoacoustic tests a booth of small volume sufficient to accomodate one subject suggests itself, since larger closed cavities require greater

*Professor
†Ph.D. Candidate

power input to obtain equivalent-amplitude waves. Such a closed chamber is conveniently driven by a group of loudspeakers located in one or more walls. By proper selection of the loudspeakers and booth volume, and special electronic compensation, the pressure-time history in the chamber can be made to simulate a sonic boom quite well, as demonstrated by previous research[3]. The procedure is, however, considerably more demanding than ordinary high-fidelity techniques. The loudspeaker-driven booth is very attractive as compared to other sonic-boom simulators in its ability to readily mimic arbitrary pressure signatures by inexpensive means.

The UTIAS sonic-boom simulation booth consists of a nearly air-tight 2.1 m^3 volume chamber driven by twelve loudspeakers mounted in apertures in one wall (Figs. 1,2). The booth features a double-wall

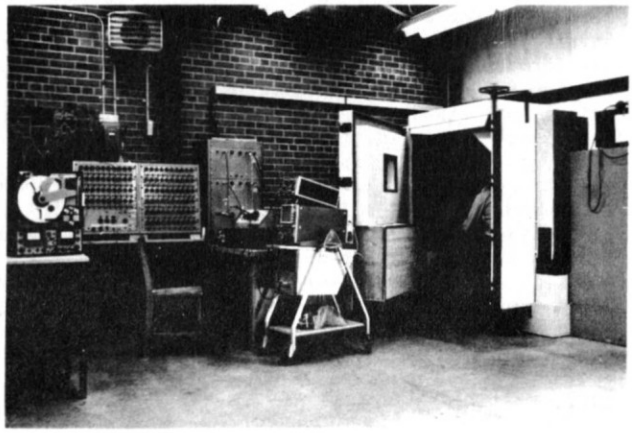

Figure 1. View of loudspeaker-driven booth showing specially-designed 100-segment function generator and other electronics.

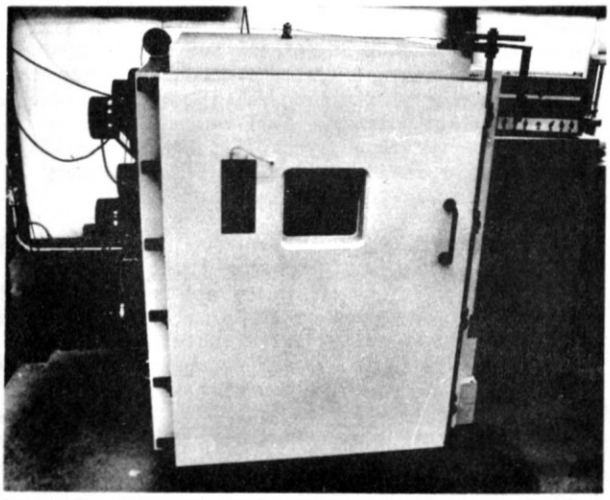

Figure 2. View of loudspeaker-driven booth showing low and high-frequency loudspeakers.

plywood construction with inside wall surfaces heavily lined with sound-absorbing fiberglass material to minimize high-frequency reflections and consequent resonances; the free-air volume is thus reduced to about 1.3 m^3. The booth interior is equipped with an illumination light, subject seat, intercom, radio, and emergency escape door handle. Six low-frequency response loudspeakers (Altec Lansing woofers, Model 515B, 38 cm diam) and six medium-high frequency response speakers (Radio Speakers of Canada, Model MF-8, 20 cm diam) are used with a cross-over network at 500 Hz; they jointly cover the frequency range from 0.1 to 5000 Hz or more required for sonic-boom simulation. As a prerequisite to reproduce the infrasonic range below 20 Hz the booth is designed to be nearly air tight, with a means for ventilation between tests. The seating arrangement is such that the head position of different height subjects would be maintained in a reasonably fixed position of known calibration, with respect to the internal booth geometry.

The electronic system that generates the input signal to the loudspeakers consists of a specially-designed 100-segment arbitrary-function generator, equalizing and cross-over networks, and three 100 W amplifiers with response down to dc. In addition, the facility has a storage oscilloscope (Tetronix 5103N/D13) and a Bruel and Kjaer condenser microphone (2.5 cm diam diaphragm), that has a flat frequency response from 0.1 Hz to 20 kHz. A schematic diagram of the electronic system and booth is shown in Fig. 3.

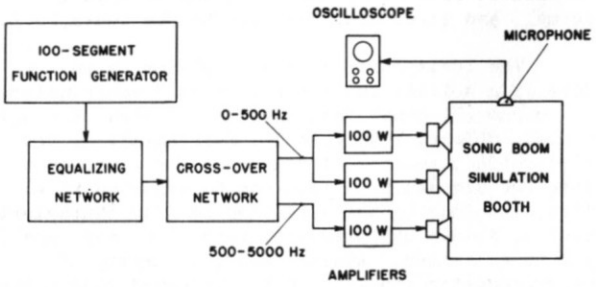

Figure 3. Electronic system for loudspeaker-driven booth.

The cross-over network separates and directs the low and high-frequency parts of the signal to the large and small loudspeakers, respectively. The equalizing network is built around an Altec Lansing Model 729A 'Acousta-Voicette' containing twenty-four 1/3-octave filters centered at frequencies from 12,500 Hz down to 63 Hz. The filter cuts off at about 8 Hz at the low end; hence, it has been necessary to add an adjustable low-pass filter (e.g., dc to 60 Hz) via a summation circuit such that the combined response goes down to dc. Individual adjustment of these twenty-four filters can compensate for a major part of the uneven frequency response of the loudspeakers and booth and hence eliminate much of the waveform distortion.

The filters are not sufficiently numerous nor of sufficient adjustment range to eliminate all of the peakiness in the frequency response; moreover, there are phase distortion effects: these jointly produce a residual distortion in the booth pressure signature. As a final 'fine tuning' to compensate for this distortion it is planned to utilize a specified counter-distortion of the input signal. The theory of this predistortion technique is as follows.

Let the input electrical signal to the booth electronics be $n(t)$ (e.g., an N-wave) and the output signal from the microphone in the booth (with assumed flat frequency response over the desired range) be $p(t)$; let their respective amplitude spectra (Fourier transforms) be $N(\omega)$ and $P(\omega)$, respectively; and let $G(\omega)$ be the effective overall frequency response of the system (treated as linear), including equalizing network, amplifiers (flat response), loudspeakers,

and booth resonances. N, P, and G are in general complex, carrying phase information. Then

$$P(\omega) = G(\omega)\, N(\omega) \qquad (1)$$

so that $P(\omega)$ replicates $N(\omega)$ only if the frequency response $G(\omega)$ is a real constant (flat response). In this special case the overpressure signature $p(t)$ in the booth faithfully mimics the input signal $n(t)$, as follows from taking the inverse Fourier transforms.

Consider now the general case of a nonflat frequency response $G(\omega)$. Choose a new input $n'(t)$ whose spectrum is $N(\omega)/G(\omega)$. Then the new pressure signature in the booth will be $p'(t)$, with spectrum

$$P(\omega) = \frac{N(\omega)}{G(\omega)}\, G(\omega) = N(\omega). \qquad (2)$$

The new pressure signature is thus an undistorted N-wave, and the corresponding input signature $n'(t)$ is a signal correctly predistorted to achieve this.

A computerized procedure can be set up for obtaining the predistorted input signal $n'(t)$. The input and output signals $n(t)$ and $p(t)$ associated with Eq. 1 are digitized by an A/D converter and processed by a fast Fourier transform program to yield $N(\omega)$ and $P(\omega)$, respectively, their inverse ratio $G(\omega)$, and the new input spectrum $N(\omega)/G(\omega)$. An inverse Fourier transform then yields the predistorted input signature $n'(t)$ as a computer output. This scheme requires special care for implementation with N-waves and similar signatures: digitization-induced errors associated with the multiple zeros of $N(\omega)$ and $P(\omega)$ lead to high amplitude 'noise' in $G(\omega)$ and hence in $n'(t)$. Additionally, iteration will be required because of the nonlinearity of the loudspeakers: $G(\omega)$ depends on the input waveform.

For use with the booth the predistorted input $n'(t)$ must be developed in terms of voltage versus time. To this end there was developed at UTIAS an elaborate electronic function generator. This analog facility has the capability of fitting, within limits, an arbitrary voltage signature $n'(t)$ by means of 100 straight line segments; the 100-slopes are adjustable by individual knobs (Fig. 1). The predistorted signal $n'(t)$ can be computed by the procedure described above; alternatively, the signal can be obtained by a trial and error process of adjusting the 100 knobs until the output pressure signature is acceptable. Both approaches for the preliminary results reported herein have been tried, and the trial and error process has been the more successful in these early results.

The 100-slope function generator, although highly flexible, involves a very laborious process for dialing in the predistorted signal, partly because of a problem with voltage drift and residual noise. It would be far simpler if the computer output for the predistorted input $n'(t)$ could go directly onto magnetic tape via a D/A converter; this entails a relatively fast computer. A digital function generator of this kind will be one feature of a computerized data-processing system that is in process of acquisition.

The capacity of the loudspeakers and amplifiers were choosen to permit peak wave-overpressures up to 300 N/m^2 for short durations (100 msec) and less than this for longer duration waves (e.g., up to 500 msec) which are limited by slight air leakage from the booth interior. Currently, overpressures up to 200 N/m^2 have been achieved. To date, rise times on the simulated sonic booms have been as low as 1 msec (at 100 N/m^2 overpressure and 100 msec duration).

Performance

Some preliminary examples of sonic-boom overpressure signatures in the loudspeaker-driven booth are given in this section. The records were taken with the booth empty and the microphone positioned on top of the seat rest. The multiple-filter equalization network was adjusted to give frequency response flat within about ±1/2 dB from about 1 to 1000 Hz. The presence of a subject would yield marked alterations in effective frequency response, owing to diffraction and changes in free-air volume and absorption; these in turn will yield distortions in the pressure signatures. But readjustment of the equalization filters can be expected to restore the essentially flat response and eliminate the distortion.

The results are displayed in Figs. 4 to 9 in the form of oscillograms. Figures 4 to 8 refer to an N-wave electrical input (ideal sonic boom), with parameters indicated in the caption. The lower trace — the 'sonic boom' signature — simulates the upper input signature quite well for the low amplitude, short duration cases (Figs. 4,5). The small irregularities reflect corresponding small irregularities in the frequency-phase response. Such irregularities are, however, typical of real sonic boom records. The short rise time (1 msec) in the simulated boom mimics the rise time of the input signature quite well.

The more powerful simulated boom of Fig. 6 at 116 N/m^2 peak overpressure is typical in amplitude of an SST in cruise, but in duration (100 msec) it is more comparable to the boom of a fighter aircraft. In Figs. 7 (weak boom) and 8 (normal boom) the duration is closer to that of an SST at 200 msec. At this increased duration the straight-line decay of the N-wave appears as an exponential decay, owing to air leakage from the booth. It is believed that an integrating circuit can correct this distortion, at least for the lower amplitudes for which the woofer will not bottom.

Finally, in Fig. 9 the ability of the booth to reproduce a special sawtooth transient[3] is shown.

In all of the above the simulated boom rise times showed no measurable difference from the 1 msec rise time (its minimum) of the electrical N-wave input from the function generator; this lies in the range of values for actual sonic booms. (Shorter boom rise times may be expected in the future when this limitation on the function generator is relaxed.) Other aspects of signature simulation seem good at the shorter duration (100 msec), but booth leakage causes a distortion (probably unimportant in subjective response) at the longer duration (200 msec).

III. The Travelling-Wave Horn

Description

The travelling-wave horn-type sonic-boom simulator consists essentially of an air compressor, storage tanks or reservoir, sonic-boom generator in the form of either a shock-tube driver (short-duration booms) or a gas reservoir with a fast-acting

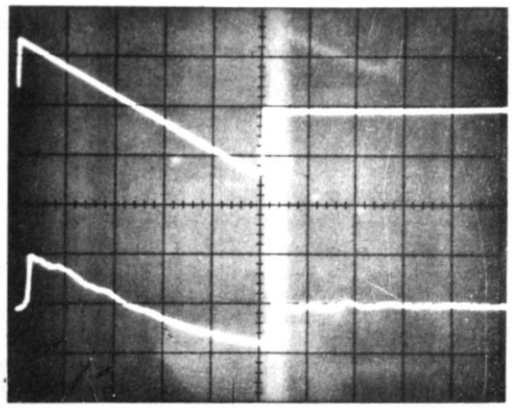

Figure 4.

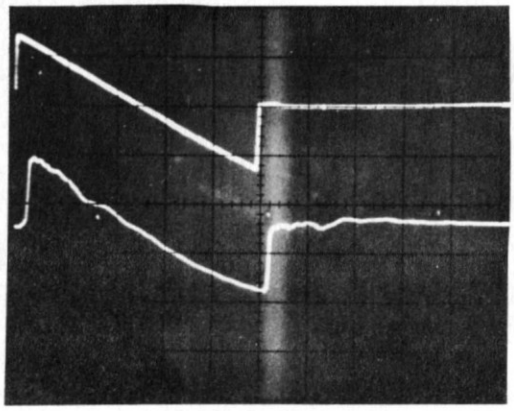

Figure 5.

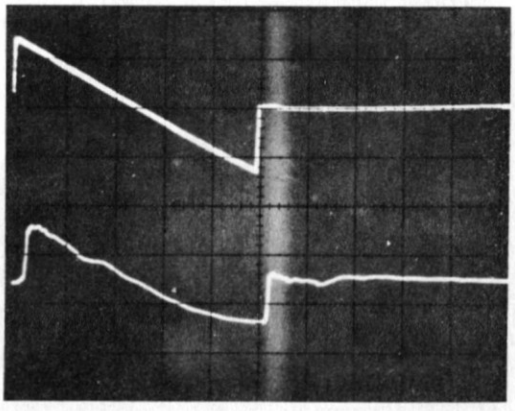

Figure 6.

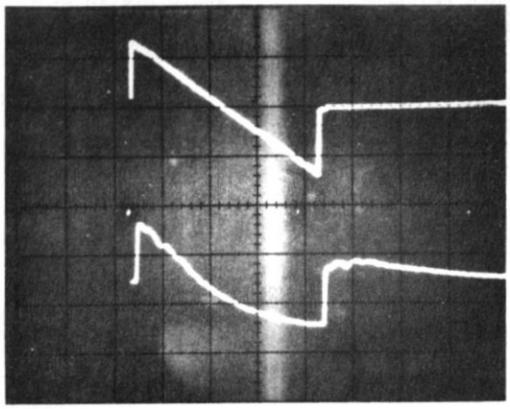

Figure 7.

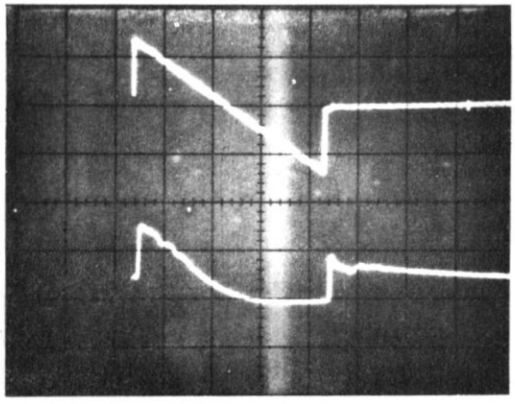

Figure 8.

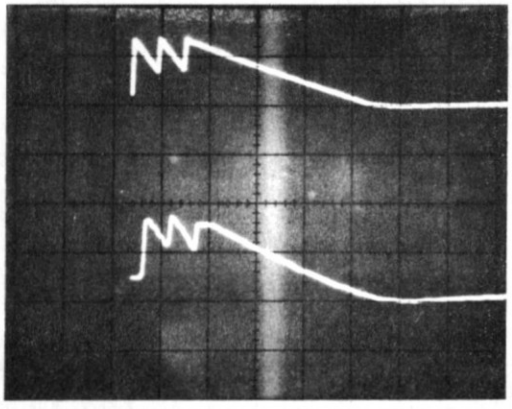

Figure 9.

Figures 4 to 8. Simulation of sonic boom 'N-wave' in loudspeaker-driven booth. Top trace: electrical input; Bottom trace: microphone over-pressure signal.

Figure 9. Simulation of special sawtooth transient of Shepherd and Sutherland[3].

Figure	Peak Overpressure (N/m^2)	Duration (msec)
4	24.7	100
5	33.4	100
6	116.0	100
7	26.7	200
8	98.0	200
9	98.0	100

mass flow valve (long-duration booms), a large pyramidal horn with an interior test section, jet-noise absorber, porous-piston-type reflection eliminator, and psychoacoustic test room. The facility is shown schematically in Fig. 10, which gives a plan view of the newly constructed UTIAS sonic-boom laboratory. The following is a description of the more important facility elements and their relevant functions.

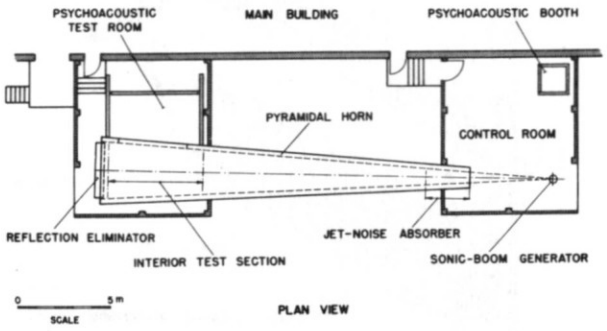

Figure 10. Sonic-boom laboratory illustrating main elements of travelling N-wave simulator.

The simulator horn is a pyramidal structure 24.4 m in length and has a 3.0 by 3.0 m open base. The first 4 m from the apex is of heavy steel construction and is located in the control room, whereas the remainder is a one-piece, reinforced-concrete structure with 20 cm thick walls and terminates in a second building (Figs. 10, 11). The extremely-rigid duct walls minimize wave energy losses and wave distortion. The total divergence angle of the pyramidal horn is 7.2 degrees. The horn is essentially a solid angle of a sphere whose walls confine and efficiently direct the wave generated near the horn apex. For this reason, the required source energy is about three orders of magnitude less than that for a full sphere[5].

Figure 11. Travelling N-wave simulator horn.

In the shock-tube driver mode of operation three different shock-tube geometries have been considered: a pyramidal driver with a pyramidal horn of the same and different divergence angles, and a constant-area driver with a pyramidal horn (shown as inserts in Fig. 19). The method of generating a wave in the expansion horn is similar to that of a conventional shock tube: the driver, separated from the expansion horn by means of a diaphragm, is pressurized above atmospheric and on bursting the diaphragm a wave is subsequently formed that propagates down the expansion horn. The gas pressure in the driver and the driver length determine the N-wave amplitude and period. In all three cases for the UTIAS facility the wave durations are short (1 to 20 msec) as compared to actual sonic booms (80 to 350 msec) due to the short driver chambers presently available. These short-duration waves have important application for diffraction studies of sonic booms propagating over model buildings or different reduced-scale land topologies. Their short rise times (40 μsec) are also valuable for certain psychoacoustic studies. The first described driver (single divergence angle horn) generates the classical N-wave for normal simulation, whereas the other two drivers give distorted N-waves which can resemble in basic features certain focussed sonic booms. For these reasons the shock tubes can be a valuable device for sonic-boom simulation. Some substantiating theoretical and experimental results will be given in a later section.

The major driver mode for the facility is the gas reservoir with a mass flow valve. The pneumatic-operated valve was designed to give the facility the capability of generating overpressure N-waves of spatial extent or period typical of those from SST's. In the valve mode of operation an air compressor is used to pressurize (1 to 18 atm) two storage tanks or reservoirs (1.3 m^3 each) that are connected via two 10 cm diam ducts to a plenum chamber (0.008 m^3) where the valve is located that controls the mass flow such that the sonic boom is produced in the horn. A view of the reservoirs, plenum chamber, valve mechanism and small end of the horn are shown in Fig. 12, and a simplified assembly drawing of the valve mechanism is given in Fig. 13.

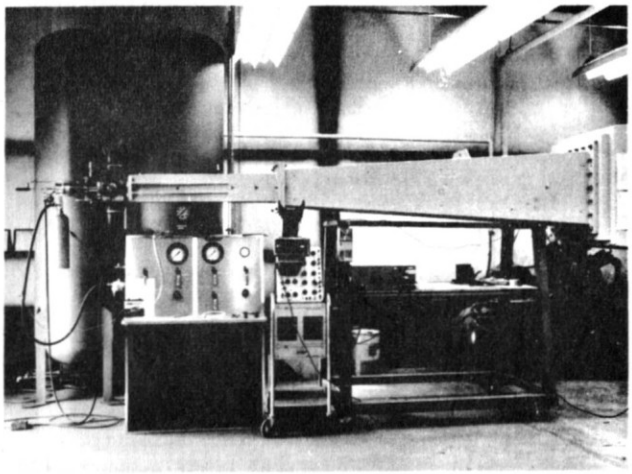

Figure 12. Control room view of horn apex, plenum chamber, mass flow valve, reservoirs, compressor, and control console.

The valve is required to pass a parabolic mass flow versus time, from zero to a maximum and back to zero again, in order to generate the N-wave. The flow area at the tapered plug corresponding to this mass flow is also a parabolic function to a first approximation. To achieve this exposed flow area, the tapered plug motion is required to be a symmetric one-cycle reciprocating movement, linear in each half of the cycle. High-pressure air from the compressor reservoir is rapidly switched, by means of an internal direction piston (activated by a solenoid valve), to either side of the large driving piston to effect the opening and closing of the valve.

The linear movement of the valve plug is

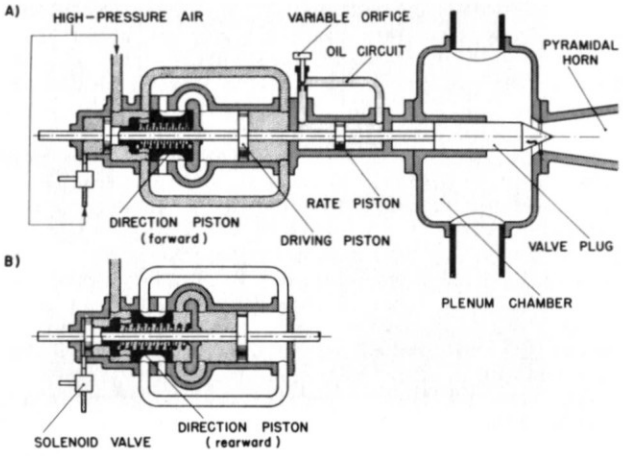

Figure 13. Assembly drawing of mass flow valve exhibiting opening (A) and closing (B) operation.

accomplished by means of the small rate piston and oil restriction orifice in the oil flow circuit. By a suitable setting of the orifice area, the oil flow is restricted to an almost constant rate, which fixes the valve plug speed and also makes it constant in each half of the cycle. The reservoir pressure, which remains essentially constant during this operation owing to its large volume, dictates the N-wave amplitude for a given duration and the open-to-close time of the valve fixes the wave duration. The existing facility exercises little control over the N-wave rise time, which is affected by the valve-plug geometry and radial position of the plug from the horn apex (presently 42 cm). The simulated N-wave has a rise time of about 3 to 4 msec which is slightly longer than that of actual sonic booms (0.1 to 2 msec in the main).

Two basic requirements of the valve are that it have sufficiently rapid operation to enable the generation of short-duration N-waves, and that it pass a large mass flow rate at the maximum valve opening to produce high-amplitude booms. An inherent characteristic of the horn-type simulator utilizing a fast-acting valve is the presence of jet noise superimposed on the generated pressure wave, as the operation is based on high-speed air flow from a reservoir. For the same mass flow rate a larger throat area gives a lower flow velocity, which results in less intense jet noise. Since with the throat area of the GASL facility[2,6] there was already a jet-noise problem, the present UTIAS facility was designed with a seven-times larger throat area of 32.3 cm^2. To further reduce the jet-noise problem an experimental study of the effectiveness of an acoustic filter was made. The filter consists of a lining on the four walls of the duct made up of 2.5 cm thick fiberglass sound-absorbing material extending from the 4.0 m to the 6.4 m station. In addition, one vertical and one horizontal panel of this material of equivalent length was installed such that the duct was divided into four equal cross-sectional areas. This absorber had the effect of reducing the jet noise markedly with negligible increase in the rise time.

A porous-piston-type reflection eliminator shown in Fig. 14, based on the analysis and existing design at GASL[2], is used to reduce echoes that arise when the incident wave encounters the end of the

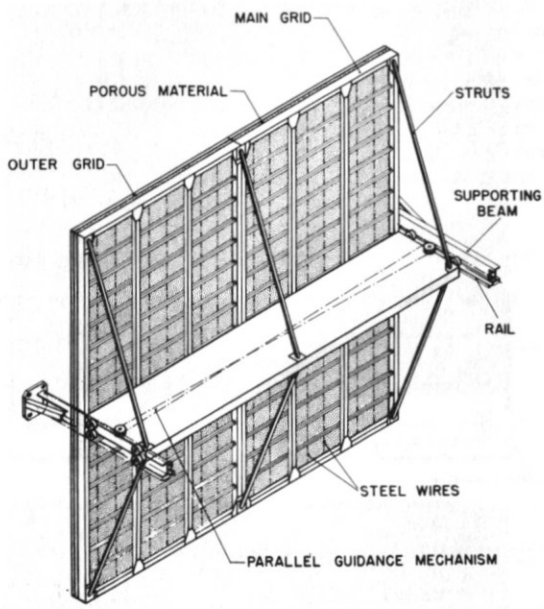

Figure 14. Porous-piston reflection eliminator

pyramidal horn. The porous piston acts essentially as a passive system matching the duct exit impedance to that of the incident wave, thereby eliminating reflections. The device rigidly supports a 2.5 cm thick microlite blanket (12 kg/m^3) that covers the horn exit area and is free to move by means of a roller and track support system. While the reflection eliminator is not required for short-duration sonic booms such as those used in diffraction studies, it is necessary for test programs involving longer duration booms to avoid echoes during testing.

In using the horn-type simulator for studies of sonic-boom propagation over different land topologies, wave diffraction over and into model buildings, and physiological and psychoacoustic response, the models or subjects can be put directly in the horn test section near the reflection eliminator. To facilitate structural response and damage studies a 1.8 by 3.6 m cutout or opening in one side wall of the duct has been designed for test panel installation. For additional psychoacoustic testing and also for room resonance studies, an adjoining full-scale test room, linked to the horn interior by the same cutout, can be suitably modified (Fig. 10). The simulator horn is easily adapted for these and other relevant research projects.

Analysis of Shock-Tube Driver Mode

The generation of N-waves to simulate the ground-intercepted sonic boom from a supersonic aircraft by means of a shock-tube driver and expansion horn having equal divergence angles is similar in process to a classical explosion. In both cases a high-pressure gas is suddenly released into a quiescent atmosphere. By examining this process, the physics of the wave formation in the horn-type simulator can be illustrated. To calculate the flow field for a weak explosion, a numerical computing procedure[7] was used to solve the one-dimensional inviscid equations of motion of continuity, momentum, and energy along with the ideal equation of state for air. An artificial viscosity technique was used to cope with shock wave motions. The results appear

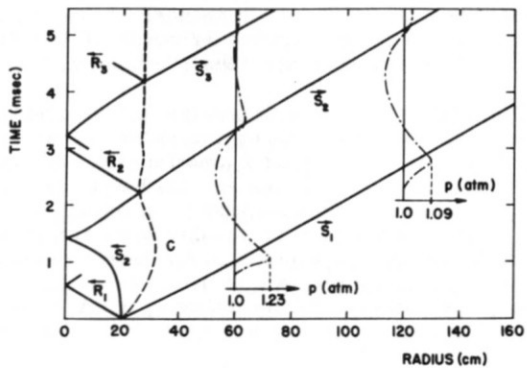

Figure 15. Numerically-computed (r,t) diagram for a weak explosion illustrating N-wave formation and propagation (p_o=4.0 atm).

in Fig. 15, in the form of an (r,t) diagram. Two overpressure traces at different fixed radii are also indicated. The paths of the various wave elements consists of a decelerating shock wave (S_1) followed by a contact surface (C) moving into the expansion horn, while a rarefaction wave (R_1) propagates into the driver gas followed by a second shock wave (S_2) at the tail of the rarefaction wave. This shock wave implodes on the origin and reflects to form the tail of the subsequent N-wave propagating down the horn. Refraction effects at the contact surface are almost negligible for this weak explosion, and additional waves (e.g., R_2, S_3, R_3) are of minor importance. The second shock wave arises as a result of the spherical nature of the flow and can be understood, as well as other parts of the flow field, by considering the motion of the contact surface. As this surface decelerates, it sends out rarefaction pulses that overtake and decrease the primary shock-wave front as well as causing the overpressure to decrease behind the front. On the other side of this surface compression waves are sent out that steepen into the shock wave. Normally, nonlinear action causes shock-wave fronts to steepen with propagation distance. However, the numerical computing scheme using a fixed artificial viscosity is inadequate in the case of weak waves, owing to the excessive spreading of the shock-wave fronts (Fig. 15).

A number of observations can be made from a study of various (r,t) diagrams for different driver-gas pressures concerning the pyramidal shock tube as a sonic-boom simulator. It becomes clear that in the case of higher driver-gas pressures the rarefaction-wave fan becomes more spread out. Consequently, the second shock wave takes longer to reach the origin and reflect resulting in an increase in the time interval (duration) between it and the primary wave. Stronger waves, which are no longer negligible, are generated by refraction at the contact surface, and the resulting wave that propagates down the horn deviates more from the desired overpressure N-wave characteristic of a sonic boom. Even though the N-wave is asymptotically formed in the far-field according to the Whitham theory[8], this result cannot be readily utilized for sonic-boom simulation purposes due to practical limitations on the horn length.

In the case of a decreasing driver-gas pressure the opposite of the above statements hold, and the generation of the N-wave becomes better. In the limiting case of a weak explosion the rarefaction-wave fan becomes very thin and is followed immediately by the second shock wave. The resulting wave in the horn, at a fixed distance, is the overpressure N-wave almost from its inception. Even in the limiting case the N-wave formation and propagation are inherently nonlinear processes. For example, the Whitham far-field asymptotic theory[8] for weak waves predicts a wavelength stretch proportional to $\sqrt{(\ln r)}$ and an amplitude decay as $1/r\sqrt{(\ln r)}$, in contrast to the linear acoustic case which predicts a fixed wavelength and the inverse-distance decay law (1/r).

The N-wave evolution and propagation processes can be solved for by numerical methods using the equations of motion directly or the characteristic equations. However, in the limiting weak wave case the linear theory (acoustic wave solution) is a good approximation for travelling-wave simulators. This theory[9] is well known and predicts the overpressure amplitude (Δp) and duration (τ_d) as given below:

$$\Delta p = \frac{\Delta p_o}{2}\frac{r_d}{r}\left[(r-at)\,H\{t_1\} - (r+at)\,H\{t_2\}\right], \qquad (3)$$

$$\tau_d = 2\,r_d/a, \quad t_1 = t-(r-r_d)/a, \quad t_2 = t-(r+r_d)/a. \qquad (4)$$

In these expressions, Δp_o, r, r_d, a, t and H{t} are initial driver-gas overpressure, radial distance, driver length, sound speed, time, and the unit step function, respectively.

The present analytical modelling of the operation of the shock-tube driven simulator brings to light many important features of the wave generation process. It provides a means of explaining the differences that always exist between experiment and the desired N-wave, for which the linear theory is inadequate. However, the linear theory has important advantages. The result is in the form of an analytical equation and usually gives a quick, inexpensive solution compared to numerical methods. A closed-form solution provides much insight into a problem by readily allowing a variation of parameters.

The linear acoustic theory has been applied successfully to other shock tube problems[10] where weak waves are generated, such as the case of a constant-area or pyramidal driver with a pyramidal expansion horn (different divergence angles in the case of the pyramidal driver). The analytical solutions and results are not reproduced here, since they require too much space. However, experimental results are given in a later section and one result is compared with linear theory.

Analysis of the Mass-Flow Driver Mode

The gasdynamic analysis for the operation of the horn-type simulator utilizing a gas reservoir with a mass flow valve has been improved and extended herein. In the initial analysis performed at GASL[2] the mass flow through the valve was assumed to model a time-varying simple point source. It is well known[11] that the simple unsteady source generates a far-field overpressure signal (Δp) proportional to the derivative of the mass flow rate ($\Delta p \sim dm/dt$). Then, if the mass flow rate (m) through the throat is parabolic with time (⌒), it follows that the overpressure distribution is the classical N-wave shape (⌐¬). The GASL analysis assumes that the simplified parabolic mass flow results from choked flow at the valve throat, controlled by means of a tapered valve plug executing a linear motion with

time (⌒).

In the present extended analysis the over-simplified simple-point-source assumption is relaxed. In addition, the flow from the valve is dealt with more realistically, partly as to the geometry of the valve opening process and partly as to the gas-dynamics. The assumed quasisteady flow through the valve, subsonic or supersonic, is ultimately matched at a certain station to the developing unsteady wave pattern. The reservoir-gas state and valve plug movement are taken as specified, and the features of the generated unsteady wave (N-wave or otherwise) are determined.

Before commencing with the analytical details let us consider a proposed model for the wave formation process in the simulator horn. This model, which has yet to be verified, is illustrated schematically in the form of an (r,t) diagram shown in Fig. 16. The flow development is very similar to

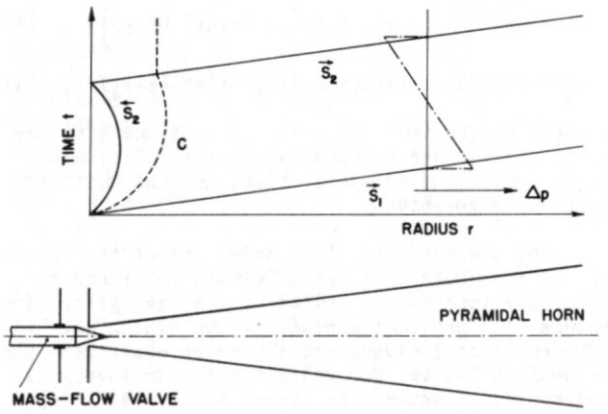

Figure 16. Proposed (r,t) diagram for N-wave formation and propagation for mass-flow-valve driver mode.

that of an explosion (Fig. 15). A primary shock wave (S_1) followed by a contact surface (C) propagates into the horn. A second upstream-facing shock wave (S_2), which is formed to match the pressure conditions in the horn, moves away and towards the valve plug where it finally reflects to become the tail of the subsequent N-wave. Other waves generated by refraction at the contact surface are weaker and of minor importance. As with the shock-tube driver, the wave formation and propagation are inherently nonlinear processes; the nonlinearity gives rise to a wave stretch and an associated amplitude decay. Although a numerical analysis exhibits these nonlinear aspects, a simple analytical solution is also desirable.

Three main assumptions are made in the analysis to simplify the wave formation and propagation processes. First, the gas flow from the reservoir to the upstream-facing shock wave is assumed to be quasisteady, so that this flow field can be determined by using a sequence of steady-state calculations. Second, the pressure and density behind the shock wave are assumed to be near atmospheric. These two conditions are sufficient to allow one-dimensional steady flow equations to determine the flow field at any instant in time. This part of the analysis gives the flow velocity behind the upstream-facing shock wave. Third, the acoustic equations are assumed to be applicable to the unsteady wave pattern in the remainder of the horn. The two flow fields are matched by means of the flow (particle) velocity at their common boundary.

The quasisteady flow approximation is justified when the plug movement changes the valve throat area slowly with time. Then wave communication between the reservoir and throat area is rapid and the flow is constantly being adjusted towards a steady state process. This assumption is invalid when the valve just starts to open or close since a severe unsteady starting or stopping process occurs. As a consequence, the analysis is incapable of predicting the rise times at the front and rear of the N-wave.

The following details on throat area, mass flow rate and the unsteady acoustic wave will be needed in the analytical development of the foregoing ideas. The UTIAS facility uses a pyramid-faced plug and the throat area exposed during its motion can be approximated by four quadrilateral areas. One such area (ABCD) is shown perpendicular to the page in Fig. 17.

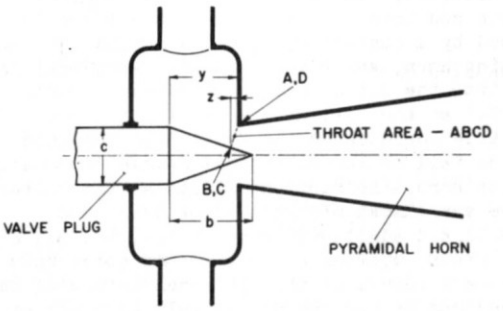

Figure 17. Valve throat area approximation.

A distance, denoted by z(t), from the horn end (AD) to the plug face (BC) is that for area ABCD to be a minimum for a plug movement y(t). In order to find z(t) and the resulting throat area $A_*(t)$ a general expression for arbitrary y(t) and z(t) is minimized with respect to z(t). The results are summarized below:

$$A_*(t) = c^2\left(2 - \frac{y-z}{b}\right)\left[\left(\frac{y-z}{b}\right)^2 + \left(\frac{2z}{c}\right)^2\right]^{\frac{1}{2}}, \quad \text{if } y-b<z<y$$
$$A_*(t) = c^2, \quad \text{if } z<y-b \tag{5}$$

where $z = (d^2 - e)^{\frac{1}{2}} - d$,

$d = (b + 4b^3/c^2 - 2\{b^2/c^2 + 1\}y)/(2 + 8b^2/c^2)$,

$e = (y^2 - by)/(1 + 4\,b^2/c^2)$.

If the plug face length (b) is long (b/c > 2), then z ≈ 0 and Eq. 5 simplifies to the following form

$$A_*(t) = c^2\,(2 - y/b)\,y/b, \quad \text{if } 0<y<b$$
$$A_*(t) = c^2, \quad \text{if } y>b \tag{6}$$

which is the desired parabolic form when y is linear with time. The existing UTIAS facility uses either of two valve plugs having values of b/c equal to 0.89 and 0.36, respectively; the first one produces a good N-wave and the latter a distorted one.

Using the one-dimensional steady flow expression for a gas discharging from a reservoir through a throat[12] and extending this theory to a quasisteady flow, the mass flow rate at the throat

$m_*(t)$ is given by the equation

$$m_*(t) = \frac{\gamma\, p_o\, M}{a_o}\left(1 + \frac{\gamma-1}{2} M^2\right)^{-\frac{\gamma+1}{2(\gamma-1)}} A_*(t) \quad (7)$$

where γ, a, p, and M are the specific heat ratio, sound speed, pressure and local flow Mach number, respectively, and the subscript 'o' refers to the reservoir gas state. In addition, the reservoir-gas (air) temperature is taken as atmospheric. The Mach number is required before the mass flow rate can be determined. For low reservoir-gas pressures ($p < 1.89$ atm), the flow at the throat is subsonic and the Mach number is given by the steady flow relation

$$M^2 = \frac{2}{\gamma-1}\left[(p_o/p_a)^{(\gamma-1)/\gamma} - 1\right] \quad (8)$$

where atmospheric pressure p_a is assumed to exist at the throat. It should be noted that for the low pressure case, the steady flow analysis does not allow an upstream-facing shock wave, and the two flow regimes are matched right at the throat. In the case of reservoir-gas pressures greater than 1.89 atm, the flow at the throat is choked and M = 1. A supersonic flow region occurs downstream of this location and is eventually terminated by an upstream-facing shock wave.

Consideration has been given to the problem of how the motion of the upstream-facing shock wave might affect the features of the generated N-wave. In general, the mass flow rate behind this shock wave is not equal to that at the throat because its motion, first away from and then back to the valve plug, affects the mass flow distribution in the horn over and above that from the valve-plug motion. To estimate the difference between these two flow-rate functions, a quasisteady flow analysis was made in which it was assumed that the shock wave instantly took the steady-flow predicted location. This analysis showed that there was a negligible difference for driver-gas pressures (1 to 18 atm) and wave durations (50 to 500 msec) of interest in sonic-boom simulation. Hence, it was concluded that the mass flow rate at the throat and behind the upstream-facing shock wave are approximately equal and that the N-wave is not affected by the shock wave movement. The above mentioned analysis[13], although not difficult, is rather long and is not reproduced here.

The flow velocity u(t) behind the upstream-facing shock wave ($p_o > 1.89$ atm) or at the valve throat ($p_o < 1.89$ atm), which is required as a boundary condition for the acoustic field, is then given from the mass-flow-rate equation in the form

$$u(t) = m_*(t)/\rho_a\, A(t) \quad (9)$$

where A(t) is the area at which the upstream-facing shock wave is located if it exists or else is the throat area and ρ_a is atmospheric density. For the UTIAS facility the area and radial distance of the horn are related by the expression $A = (r/8)^2$.

The acoustic field is governed by the spherically symmetric wave equation

$$a^2 \frac{\partial^2(r\phi)}{\partial r^2} = \frac{\partial^2(r\phi)}{\partial t^2} \quad (10)$$

where ϕ is a velocity potential function. For outgoing waves only, the solution to this equation is

$$\phi = \frac{1}{r} f(t-r/a) \equiv \frac{1}{r} f(\tau). \quad (11)$$

The overpressure (Δp) and particle velocity (Δu) are related to the velocity potential by the expressions:

$$\Delta p = -\rho_a \frac{\partial \phi}{\partial t} = -\frac{\rho_a}{r} f'(\tau) \quad (12)$$

$$\Delta u = \frac{\partial \phi}{\partial r} = -\frac{1}{ar} f'(\tau) - \frac{1}{r^2} f(\tau) \quad (13)$$

where the prime (') denotes differentiation with respect to τ.

If the particle and flow velocities were equated directly by using Eqs. 9 and 13, a nonlinear differential equation in the unknown $f(\tau)$ would result because the radius for matching the velocities is not constant. To make the problem more tractable this radius for matching is assumed constant and equal to the valve plug location denoted by r_v. This particular choice was made for the following reason. It can be shown that the value of r_v affects mainly the rise time at the head and tail of the N-wave. Since the analysis is incapable of predicting these, the choice of r_v is arbitrary and is chosen such that agreement with experiment is obtained in terms of rise times. Then a simple first-order ordinary differential equation in terms of the potential signature $f(\tau)$ is obtained, with the mass flow rate acting as a forcing function:

$$f'(\tau) + \frac{a}{r_v} f(\tau) = -\frac{64\, a}{\rho_a r_v} m_*(\tau). \quad (14)$$

Once $f(\tau)$ is solved for the overpressure and particle velocity are found by means of Eqs. 12 and 13.

The $f'(\tau)$ term corresponds to the acoustic far field; it is normally negligible compared with the term $af(\tau)/r_v$. However, when $m_*(\tau)$ changes rapidly (large m_*') this term can become dominant. If this term is neglected the overpressure can then be related directly to the derivative of the mass flow rate by using Eq. 12:

$$\Delta p = 64\, m_*'(\tau)/r. \quad (15)$$

This is the relation used by GASL[2] and discussed in the first paragraph; it is equivalent to that for an unsteady simple source[11](small pulsating sphere). Equation 15 for the overpressure signature does not contain the arbitrary parameter r_v and is very convenient for a quick analysis. However, wave rise times due to the r_v term are lost. The examples which follow illustrate this.

Solutions to the full Eq. 14 can be obtained in analytical form for simple mass-flow distributions. However, in more complex cases the use of a numerical procedure is more convient, and at times necessary, to obtain a solution. The simple-point-source approximation, Eq. 15, can be solved analytically. In all of the following examples the valve-plug motion y(t) is taken as linear with time as shown in Fig. 18(a). As a first analytical example, consider the plug motion to give a parabolic area with time as given by Eq. 6 (limiting case of the more general area expression of Eq. 5). The mass flow rate is of similar parabolic form and given by

$$m_*(\tau) = 4\,\bar{m}_*\,(1 - \tau/\tau_d)\,\tau/\tau_d, \qquad 0<\tau<\tau_d$$
$$m_*(\tau) = 0, \qquad \tau<0,\ \tau>\tau_d \quad (16)$$

where $\bar{m}_*$ is the maximum mass flow rate and τ_d is the wave duration. Equation 15 (simple point source) then gives the exact N-wave overpressure signature as follows

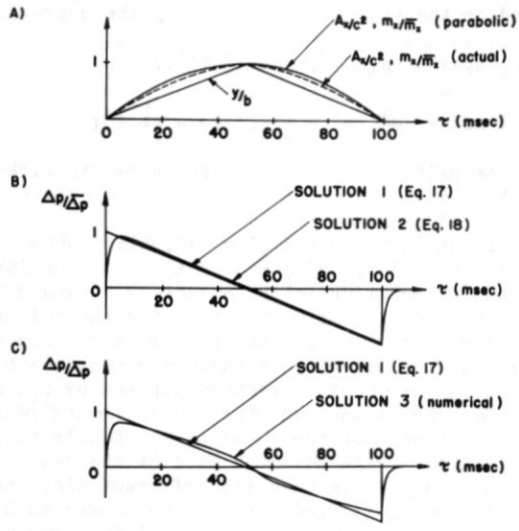

Figure 18. Predicted valve area, mass flow rate, and N-wave overpressure signatures for a linear valve plug movement.

$$\Delta p = \overline{\Delta p}\,(1 - 2\tau/\tau_d), \qquad 0<\tau<\tau_d$$
$$\Delta p = 0, \qquad \tau<0,\ \tau>\tau_d \tag{17}$$

where $\overline{\Delta p} = 256\ \overline{m}_*/(r\ \tau_d)$ is the maximum overpressure of the N-wave. It should be noted that for equivalent-amplitude waves, longer durations imply larger mass flow rates. These can be obtained by using higher reservoir-gas pressures or larger throat areas.

The more accurate Eq. 14 can also be solved analytically for the parabolic mass-flow-rate case. The results are given by the following expressions:

$$\Delta p = \overline{\Delta p}\left[h\left(1 - \exp\{\frac{-a\tau}{r_v}\}\right) - 2\tau/\tau_d\right], \qquad 0<\tau<\tau_d$$
$$\Delta p = \overline{\Delta p}\left[h\left(1-\exp\{\frac{-a\tau_d}{r_v}\}\right)-2\right]\exp\left[\frac{-a(\tau-\tau_d)}{r_v}\right], \qquad \tau>\tau_d \tag{18}$$

where $h = (1 + 2r_v/\{a\ \tau_d\})$. The exponential terms, with short time constants (r_v/a arbitrarily taken as 1.3 msec), give the rise times on the front and rear of the N-wave. This expression reduces to that for the exact N-wave (Eq. 17) as $r_v \rightarrow 0$. The two overpressure signature results given by Eqs. 17 and 18 and denoted as Solutions 1 and 2, respectively, are shown in Fig. 18(b). The N-wave duration is 100 msec.

For the last example (denoted Solution 3), the exact area expression (Eq. 5) is used and Eq. 14 is solved by a simple numerical method. The actual area distribution and resulting mass flow rate for this example are shown in Fig. 18(a), and the overpressure signature appears in Fig. 18(c). For this example the length of the tapered portion of the valve plug was specified as b = 0.89c, a moderate length.

The differences between the actual mass flow rate (finite plug length of b = 0.89c) and the parabolic mass flow rate (very long, slender plug) is small (about 10%). Correspondingly, the resulting overpressure signature is distorted slightly from the ideal N-wave as illustrated. However, in the case of a more blunt valve plug (b < 0.89c) the differences in the throat area, mass flow rate, and overpressure distributions for the parabolic and actual cases become more pronounced. Solution 1, with zero rise time, always predicts the highest peak overpressure. The difference in peak values between Solutions 1 and 2 is 10 percent in the case of a 100 msec N-wave. This difference increases for shorter duration N-waves (15% for 50 msec) and decreases for longer duration N-waves (2% for 400 msec). There is a further decrease in peak overpressure from Solutions 2 to 3 and this is about 10 percent and remains nearly constant for all N-wave durations. The latter decrease is due to the valve plug; shorter taper lengths give lower amplitude N-waves. Hence, the peak overpressure performance of the facility is decreased by using too short a plug-face length, and in addition the waveform is distorted from the desired N-wave shape.

Some Experimental Results

The results for the shock-tube mode of operation of the horn-type simulator are presented first and those for the reservoir-gas driver and the mass flow valve mode follow. Since the present shock tubes have short driver-chambers, short-duration waves (1 to 20 msec) are produced. The primary importance of these waves is in their application for diffraction studies of sonic booms propagating over and into model buildings, or over different reduced-scale land topologies. Short-duration signals are required to provide correct geometric scaling (e.g., a building 30 m in height and actual sonic boom of 250 msec duration could be scaled down to a model 30 cm in height and a signal 2.5 msec in duration). In addition, the short rise times (40 μsec) of these booms are valuable for certain psychoacoustic and physiological studies, since subjective loudness of the sonic boom and thus startle effects are dependent mainly on rise time and peak overpressure, and not on duration. The classical N-wave for these studies can be simulated quite well by using a pyramidal shock tube. In addition, consideration has also been given to simulating focussed sonic booms that occur when aircraft accelerate or maneuver. Driving chambers of suitable geometry were used to generate overpressure waves similar to certain focussed sonic booms.

A typical short-duration N-wave is shown in Fig. 19(a); it was generated by a pyramidal shock tube (shown as an insert in the figure) having a driver and expansion section of the same divergence angle. The N-wave rise times (not indicated) are very short (40 μsec). The continuous overpressure decrease from the N-wave head to the tail is not quite linear, as desired for sonic-boom simulation, but this becomes more linear for the case of lower driver-gas pressures (p_o<2.4 atm). For higher pressures the higher amplitude wave wave becomes more distorted from the N-wave shape (see previous comments on the explosion example) and is not too useful for N-wave simulation. Longer duration N-waves can be obtained by using longer driver lengths. Detailed work is not presented here since quite extensive studies can be found in the literature[14,15].

The focussed sonic booms of Refs. 15 and 16 is essentially typified by a wave front that is two-to-three times larger in amplitude than the tail wave. The fall in overpressure between the head and tail is rapid at first and then more slowly, ending with an

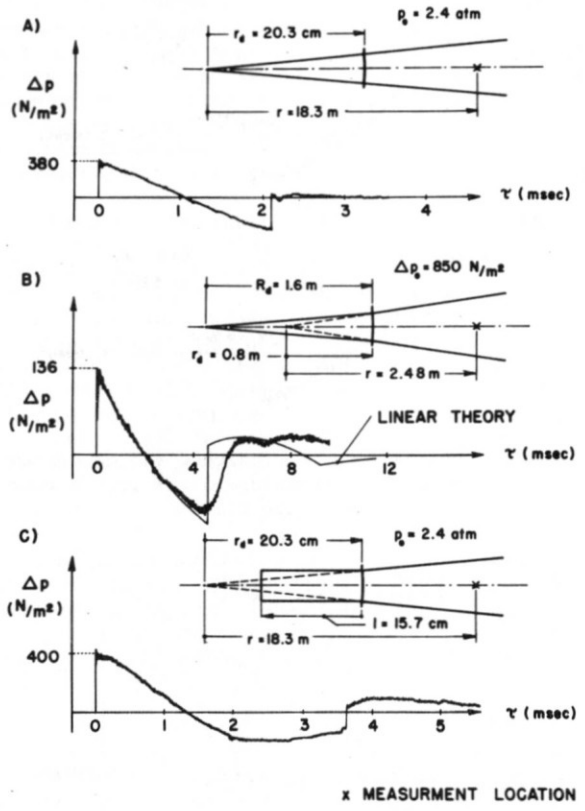

Figure 19. Shock-tube generated N-wave and simulated focussed booms (experimental waveform in Case (b) is from Ref. 14).

almost constant pressure region just ahead of the tail shock wave. Two different shock-tube geometries could simulate focussed booms. The first, having a pyramidal driver with a divergence angle of about one-half that for the expansion horn, generates a wave similar to a focussed boom (Fig. 19(b)). The rapid fall in overpressure behind the wave front is achieved, but the constant-pressure portion is quite short. Also, the second shock front is not well formed. Both problems can be overcome. A longer driver, according to linear theory[10], will give a better constant-pressure portion, and a longer wave propagation distance will help in the formation of a better second shock front. Note that the linear theory predicts the waveform and amplitude quite well for this weak wave case. The second shock tube considered has a constant-area driver, having a length which is 25 percent shorter than a pyramidal driver of the same divergence angle as the horn, and it can also be used for focussed sonic-boom simulation. One example appears in Fig. 19(c). This case is more limited in its application for simulating the focussed boom. First, the rapid fall in pressure behind the primary shock front is not achieved although the pressure levels out quite well before the tail shock front. Second, the driver-gas pressure as well as the shock-tube geometry is important in the wave formation process, since nonlinear wave action is required to simulate good focussed booms. For this reason, only a small range of driver-gas pressures are available for each shock-tube geometry which can give the required nonlinear wave action. This also means that the models have to be placed at a suitable distance from the driver section in order to control the wave amplitude, since it cannot be controlled adequately by the driver-gas pressure. It can be concluded that the shock tube with a pyramidal driver of different divergence angles is most promising for simulation of focussed sonic booms of short duration (e.g., 1 to 20 msec).

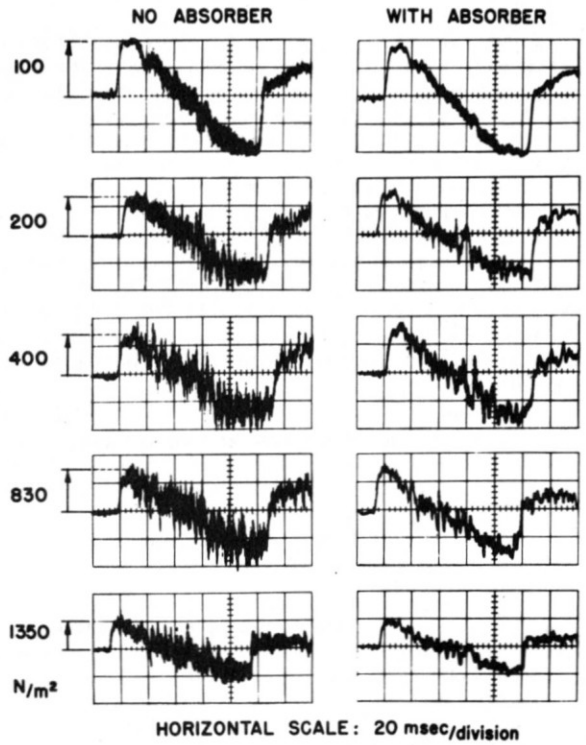

Figure 20. Simulated N-waves generated with mass-flow-valve driver with and without jet-noise absorber (reservoir driving pressures: p_o= 1.3, 2.5, 5.1, 9.2, 13.9 atm).

Some experimental results for the travelling N-wave simulator driven by means of a reservoir gas with a mass flow valve are shown in Fig. 20. The simulated sonic-boom records in the first column were obtained wihout the use of the jet-noise absorber and those in the duplicate set with the absorber. The sonic-boom records are nominally 110 msec in duration and increase in amplitude with corresponding reservoir-gas pressures of p_o/p_a = 1.3, 2.5, 5.1, 9.2, and 13.9. Wave rise times are typically 3 to 4 msec. The fall in overpressure between the head and tail of the wave is not quite linear. The levelling out in overpressure ahead of the wave tail is due to the reflected wave from the end of the horn, which tends to raise the pressure. This is also evident after the rear shock front.

The intense jet noise superimposed on the simulated booms is a problem. It increases the subjective loudness substantially and can invalidate some psychoacoustic and physiological studies. However, it is not expected to affect the response of structures, owing to their low dominant response frequencies — a mismatch. In general, the noise is less intense and not much of a problem for the shorter duration N-waves (<150 msec) and the smaller peak overpressures (<100 N/m^2) if the jet-noise absorber is utilized. For longer duration or larger amplitude N-waves the high frequency noise is greatly reduced, but substantial superimposed noise still

remains. Further noise reduction can be obtained by installing more sound-absorbing material; however, the wave amplitude begins to be reduced and, worst of all, the wave rise time increases. For further jet-noise attenuation the only alternative approach appears to be the design of a new mass flow valve that will generate less intense noise from the onset. This approach is now under consideration.

The present performance of the reflection eliminator is not entirely satisfactory. The porous piston appears to function properly, but reflection elimination is not achieved since the piston is located very close (1 m) to the building wall. The incident sonic boom interacts not only with the porous piston but also with the building wall, and together they act more like a solid wall to the incoming N-wave. The result is a reflected wave of similar profile to the incident wave. This can be observed from the waveforms shown in Fig. 21, where the reflection eliminator was used for one test and a near-rigid wall for the other. To improve the performance, the wall will have to be moved away from the horn end.

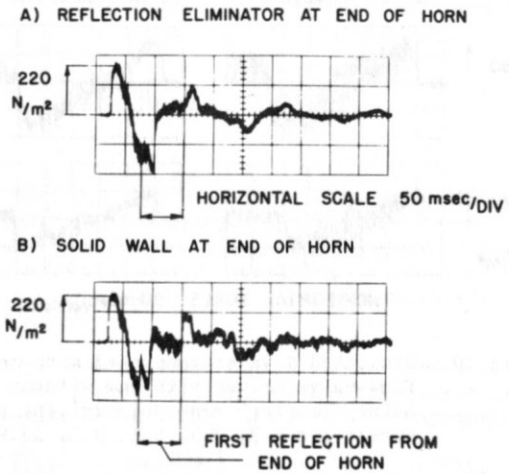

Figure 21. Comparison of reflected waves from reflection eliminator and almost rigid wall at end of horn.

Two simulated sonic-boom signatures having peak overpressures of 200 and 830 N/m^2 and durations of 110 msec are compared with those predicted by the analysis (Fig. 22). In general, the waveform and amplitude prediction for these very strong booms is good. The amplitudes of the experimental booms are generally lower but usually within 10 percent of the predicted values. There are differences in the experimental and predicted waveforms. Experimental profiles have a more rapid fall in overpressure behind the wave front. In addition, the duration of the above-atmospheric portion of the wave exceeds that for the below-atmospheric part. These characteristics are common to all the simulated booms and are not predicted by the analysis.

Further experimental and predicted results are given in Fig. 23. On this graph the N-wave amplitude is plotted versus reservoir-gas pressure for two different durations of 80 and 200 msec. These results show that the experimental values normally fall below the predicted ones but are usually within 10 percent. The agreement between experimental and predicted amplitudes becomes better for lower driver pressures and good agreement has been found

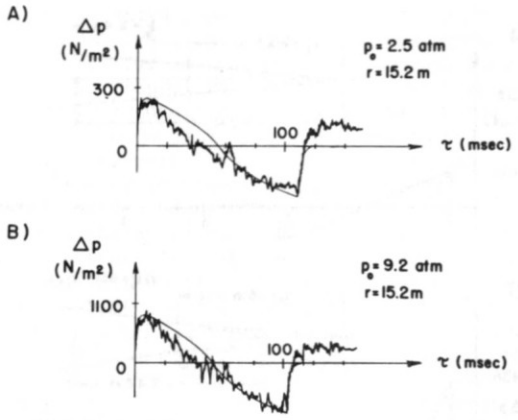

Figure 22. Comparison of predicted and experimental N-wave overpressure signatures having durations of 110 msec.

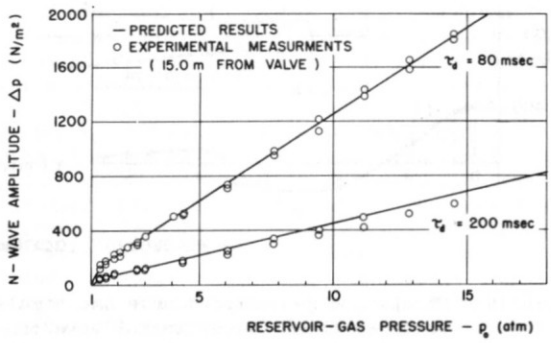

Figure 23. Predicted and experimental performance for travelling N-wave simulator: peak overpressure versus driving pressure for N-wave durations of 80 and 200 msec.

for the case where the flow is subsonic at the throat ($p_o/p_a < 1.89$). The measurement station for the experimental results was 15.2 m from the horn apex. Wave amplitudes at other stations can be obtained simply by using the acoustic decay law (1/r). This graph also illustrates that for a fixed driving pressure, longer duration N-waves result in lower amplitudes.

At UTIAS a preliminary physiological investigation[17] was made into the effects of simulated sonic booms on the temporary threshold shift in hearing, temporary increase in heart rate, and heart-rate recovery time. The tests were performed in the horn-type simulator with the jet-noise absorber installed. Eight volunteer subjects were selected from a larger group of twenty; they ranged in age from 24 to 36 years. All showed normal hearing characteristics from initial audiograms (audiograms were taken just before and after each test) and none reported any heart disorder. Each subject underwent three tests on consecutive days, being exposed to fifty sonic booms in a two minute interval for each test. Peak sonic-boom overpressures of 100, 200 and 400 N/m^2 were used in the first, second, and third tests, respectively. Heart rate measurements were recorded for the following eight events. The subject, sitting in a comfortable reclining position, was asked a simple question ("In which country were you born?"), told to perform an easy task ("Lift your left leg

till the count of ten."), and asked an elementary mathematical problem ("What is 56 divided by 8?"). Then the subject was exposed to five sonic booms. After each of these eight events, the time interval for the heart rate to return to its normal state was also monitored. Thereafter, the person was subjected to the remainder (45) of the sonic booms and heart rate measurements were not recorded, owing to the reduced startle effect through conditioning.

The simulated sonic booms in the test region of the horn had rise times of 3 to 4 msec, durations of 80 msec, and some residual jet noise. It was found by calculation[17] that the combined sonic boom and jet noise had loudness ratings of 220, 330, and 510 sones for the test overpressures of 100, 200, and 400 N/m^2. These are comparable to loudness ratings of 220, 310, and 480 sones for equivalent-amplitude sonic booms free of jet noise and having a rise time of only 0.1 msec. The effect of the jet noise is thus an increase in the subjective loudness, thereby making the simulated sonic booms comparable in loudness rating to 'noise free' booms having a shorter rise time. For comparison, sonic booms generated by the Concorde can have rise times as short as 0.1 msec in extreme cases[15] (typically 0.1 to 2 msec). Hence, the simulated booms are comparable or more severe in loudness than actual sonic booms. For this reason the physiological results to be given are thought to be indicative of response to actual booms.

The audiogram results showed that none of the subjects suffered a serious temporary shift in hearing, even in the most severe case when peak overpressures were 400 N/m^2. Threshold shifts of up to 10 dB did occur in a few tests, but these are small and within safety limits[18]. The electrocardiogram results indicated that subjects showed a classical heart-rate startle effect, even in the case of moderate peak overpressures (100 N/m^2) of the order of those produced by an SST. Heart rate increases were small with the largest recorded increase of 20 percent. Normally, the first of the five sonic booms gave the largest increase which was usually less than a 10 percent change. It was found that the time interval for the heart rate to return to normal from the startle effect could be as long as 25 seconds but typically took less than 10 seconds. Similar heart rate increases and recovery times occurred when the subjects answered the two questions. In the case of the subjects raising their leg, the heart rate increase was slightly larger (normally less than 20 percent) and the recovery time was generally less than 20 seconds. Since heart rate increase and recovery time due to the sonic-boom disturbance and the normal question and command stimuli are similar, actual sonic booms should not produce significant heart rate changes and recovery times in normal human beings.

Even though heart rate change and temporary threshold shift in hearing due to the sonic-boom disturbance are not significant, other physiological responses could be important. In addition, psychoacoustic response could also be significant.

A psychoacoustic study[19] has been completed in the horn facility in which the effect of the sonic boom on an automobile driver was examined. The subject performed a tracking task which simulated the control of a vehicle on a road with a fixed crown — an unstable situation — with random disturbances playing the role of road irregularities.

An important function of the facility is to conduct structural studies (wall panels, window response, room resonance). For such problems the jet noise is not expected to interfere. An investigation of the sonic boom effects on partially-fatigued wall panels is in progress[20]. These studies are directed at gathering response and damage data in order that criteria can be established to assist with citizen damage claims arising from SST overflights in the Canadian context. In addition, a study of the distortion of a short-duration N-wave (2 to 5 msec) owing to frequency-dependent refraction during propagation through an air jet is in progress.

IV. Concluding Remarks

The motivation, design, theory, and initial performance of two Canadian sonic-boom simulation facilities — a loudspeaker-driven booth and a large travelling-wave horn — have been reported. Early performance and some research results were sketched, and the potential for a variety of future investigations was indicated. The horn and booth-type simulators complement each other to provide flexibility for the study of human, animal, and structural response to the sonic boom.

V. Acknowledgements

The authors are indebted to a number of people who have been very helpful during the establishment phase of the sonic-boom simulation facilities located at the University of Toronto, Institute for Aerospace Studies. Our thanks are extended to the following: Dr. G.N. Patterson (Director, UTIAS), Dean J.M. Ham (UT), Dr. G. de B. Robinson (UT), Mr. F.R. Thurston (National Aeronautical Establishment); Mr. C.C. Halton, Mr. J. Gratwich, Mr. G. Skinner, Mr. P. Eggleton, and Mr. M.E. Brenckmann (all of the Ministry of Transport, Canada); Mr. I.S. Macdonald (Air Canada), Mr. I.R. Schwartz (National Aeronautics and Space Administration, USA), Mr. L.J. Gale (General Applied Science Laboratories, New York, USA); Dr. J. Locke, Dr. L.D. Reid, and Dr. R.C. Tennyson (all of UTIAS). The facility design contributions by Dr. A. Palm-Leis, Mr. W. Czerwinski, Mr. A. Perrin, Mr. A. Falkiewicz, and Mr. K.A. Leung are appreciated. In this connection reference can be made to the UTIAS Annual Progress Reports for 1969-1971. The technical work of Mr. H. Schumacher, Mr. M. Millan, and Mr. G. Sachade is also gratefully acknowledged.

The financial support received from the Canadian Transport Commission, the Canadian Air Transportation Administration, the Canadian Transportation Development Agency, the National Aeronautical Establishment of the National Research Council (Canada), and Air Canada is acknowledged with thanks.

VI. References

(1) Glass, I.I. and Wada, I., 'A Preliminary Investigation of Sonic Boom Problems,' UTIAS Progress Report, 1969, p. 26.

(2) Tamboulian, R., 'Research and Development of Sonic Boom Simulation Device,' GASL TR No. 713, 1968.

(3) Shepherd, L.J. and Sutherland, W.W., 'Relative Annoyance and Loudness Judgements of Various Simulated Sonic Boom Waveforms,' NASA CR-1192, 1968.

(4) Berry, B.F., 'The Simulation of Sonic Boom in a Pressure Chamber,' M.Sc. Thesis, Institute of Sound and Vibration Research, Univ. of Southampton, 1969.

(5) Glass, I.I., 'Aerodynamics of Blasts,' UTIA Review No. 17, Univ. of Toronto, 1960, p. 24 (see also Can. Aero. J., Vol. 7, No. 3, 1961, pp. 109-135).

(6) Tamboulian, R. and Peschke, W., 'Description and Capabilities of a Travelling Wave Sonic Boom Simulator,' NASA CR-1696, 1970.

(7) Brode, H.L., Asano, W., Plemmons, M., Scantlin, L. and Stevenson, A., 'A Program for Calculating Radiation Flow and Hydrodynamic Motion,' Memorandum RM-5187-PR, Rand Corporation, 1967.

(8) Whitham, G.B., 'On the Propagation of Weak Waves,' J. Fluid Mech., Vol. 1, Part 3, 1956, pp. 290-310.

(9) Jeffreys, H. and Jeffreys, B.S., 'Methods of Mathematical Physics,' Cambridge Univ. Press, Ed. 3, New York, 1956, pp. 560-561.

(10) Gottlieb, J.J., 'Theoretical and Experimental Aspects of Sonic-Boom Simulation using Shock Tubes,' UTIAS Report (to be published).

(11) Morse, P.M. and Ingard, K.U., 'Theoretical Acoustics,' McGraw-Hill, 1958, pp. 309-310.

(12) Shapiro, A.H., 'The Dynamics and Thermodynamics of Compressible Fluid Flow,' Ronald Press Co., New York, Vol. 1, 1953, p. 85.

(13) Gottlieb, J.J., 'Sonic-Boom Simulation in a Travelling N-Wave Facility,' UTIAS Report (to be published).

(14) Peter, A. and Brunner, J.J., 'Etude d'un Tube à Choc de Forme Pyramidale pour la Génération d'une Onde en N,' T11/70, Institut Franco-Allemand, de Recherches de Saint-Louis, 1970.

(15) Thery, C., Peter, A. and Schlosser, F., 'Le Générateur de Bang de l'ISL,' Report No. 15/71, Institut Franco-Allemand, de Recherches de Saint-Louis, 1971.

(16) Wanner, M.I.C., 'Essais Mirage IV,' Aircraft Engine Noise and Sonic Boom, AGARD CP No. 42, May 1969.

(17) Carothers, R., 'Initial Calibration and Physiological Response Data for the Travelling-Wave Sonic-Boom Simulator,' M.A.Sc. Thesis, University of Toronto (to be published).

(18) Coles, R.R.A., Garinther, G.R., Hodge, D.C. and Rice, C.G., 'Hazardous Exposure to Impulse Noise,' J. Acoust. Soc. Am., Vol. 43, No. 2, 1968, pp. 336-343.

(19) Lips, K., 'An Unstable Automobile-Tracking Task with a Sonic-Boom Disturbance,' UTIAS Technical Note (to be published).

(20) Leigh, B., 'Life-Time Concept for Gypsum Panels Subjected to Sonic Boom,' M.A.Sc. Thesis, University of Toronto (to be published).